

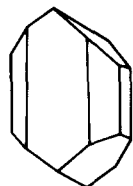
Geochemistry of the Lyngdal hyperites (S.W. Norway): comparison with the monzonorites associated with the Rogaland anorthosite complex

D. DEMAIFFE¹, B. BINGEN^{1,3}, P. WERTZ¹ and J. HERTOGEN²

¹Lab. associés de Géologie – Pétrologie – Géochronologie, CP 160, Univ. Libre de Bruxelles, 50 av. Roosevelt, B-1050 Bruxelles (Belgium)

²Afd. Fysico-chemische geologie, University of Leuven, Celestijnenlaan 200c, B-3030 Leuven (Belgium)

LITHOS



Demaiffe, D., Bingen, B., Wertz, P. and Hertogen, J., 1990. Geochemistry of the Lyngdal hyperites (S.W. Norway): comparison with the monzonorites associated with the Rogaland anorthosite complex. *Lithos*, 24: 237–250.

The Lyngdal hyperites (LYHY) crop out as two small, post-tectonic intrusions of gabbro-noritic to monzonoritic composition, at the extreme South of Norway. They display subophitic textures with plagioclase laths (An_{40} to An_{58}), orthopyroxene (En_{56} to En_{62}), clinopyroxene ($Wo_{47.5}En_{39}Fs_{13.5}$), ilmenite, magnetite and interstitial myrmekite fringes, K-feldspar, quartz, apatite and biotite. The SiO_2 content is very constant (50–53%), but K_2O ranges from 1% to 1.6% in differentiated facies. REE patterns are smooth [$(La/Yb)_n = 6$]. The hyperites define an Rb/Sr isochron of 910 ± 82 Ma (2σ), with an initial ratio of 0.7054. ϵNd is slightly positive (0 to +2) and average lead isotopic initial ratios are 17.45 [$(^{206}Pb/^{204}Pb)_i$] and 15.51 [$(^{207}Pb/^{204}Pb)_i$].

The LYHY represent magmatic liquids that have not fractionated large amounts of plagioclase. They are quite comparable to the rocks of the monzonoritic series that occur in the nearby Rogaland anorthosite complex. (1) The plagioclases have the same composition; plagioclase phenocrysts are locally present. (2) They display enrichments in TiO_2 , P_2O_5 and K_2O . (3) They have comparable REE patterns. (4) The isotopic data show that the monzonorites and the LYHY derive from the same isotopic reservoir.

The LYHY nevertheless differ from the monzonorites by their high-Al content ($Al_2O_3 = 18.5\%$) and their lower FeO_{tot} content ($FeO_{tot}/FeO_{tot} + MgO = 0.62$).

The geochemical and isotopic diversity of the monzonoritic magmatism, including the LYHY, implies that each occurrence represents a distinct magma batch generated from a distinct source. The LYHY could tentatively be interpreted as a Fe-poor (Mg-rich) end-member of the monzonoritic magmatism occurring to the East of the anorthosite complex.

(Received December 13, 1988; revised and accepted December 6, 1989)

Introduction

The Rogaland anorthosite complex (Michot, 1960; Michot and Michot, 1969; Duchesne and Michot, 1987) crops out in the core zone of the Proterozoic Sveconorwegian (= Grenvillian, 1200–900 Ma) province of S W Norway. There is mounting evidence that three distinct magmatic series are present in this complex (Duchesne et al., 1985a;

Demaiffe et al., 1986): (1) the massif-type anorthosite series of basaltic affinity, (2) the monzonoritic (= jotunitic) series and (3) the charnockitic series (Fig. 1).

With regard to rock volume, the monzonoritic series is of lesser importance. The monzonorites are interpreted as magmatic liquids on the basis of their fine-grained nature (<1 cm) compared with the massif-type anorthosites and of their field occurrence as dykes, thin intrusions and chilled margins of larger differentiated intrusions. The systematic absence of significant negative Eu-anomalies in the

³Research assistant of the Belgian National Fund for Scientific Research.

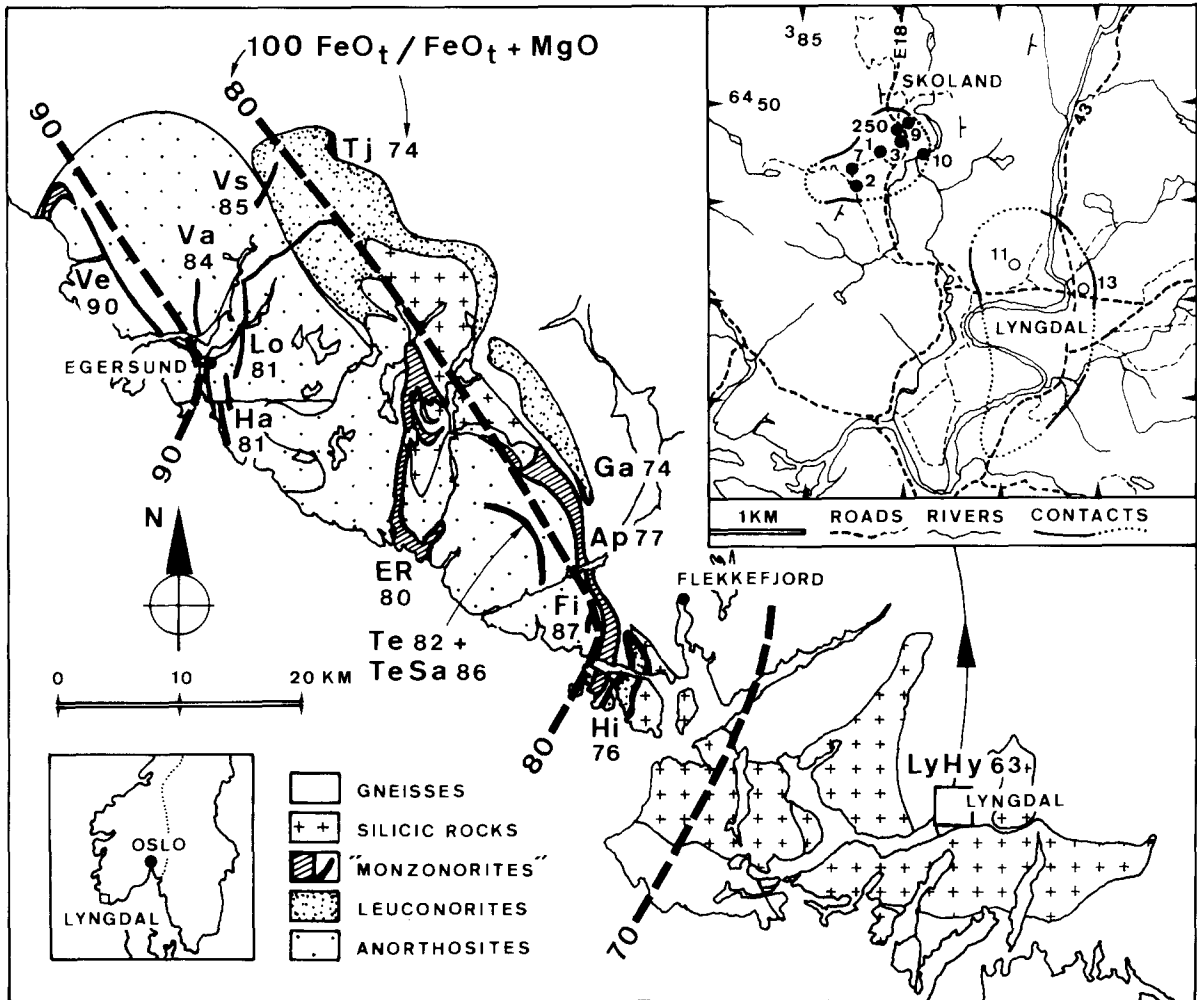


Fig. 1. Simplified geological map of the Rogaland-Vest-Agder showing the Lyngdal hyperites (LYHY) and the three magmatic series of the Rogaland anorthosite complex (from Michot and Michot, 1969; Duchesne et al., 1985a, modified): the massif-type anorthosites belong to the basaltic series, the monzonorites and associated leuconorites belong to the monzonoritic series and the silicic rocks to the charnockitic series.

The $\text{FeO}_{\text{tot}}/\text{FeO}_{\text{tot}} + \text{MgO}$ ratios of the least differentiated samples of the LYHY and of each monzonorite occurrence are plotted, showing the regional increase of this ratio towards the core zone of the anorthosite complex.

In the upper right inset: detail of the Skotland and Lyngdal hyperites with sample locations. The geological contacts of the hyperites are drawn following Lavreau (1970), Falkum et al. (1979) and personal observations.

Abbreviations for the monzonorite occurrences: *Ap*: apophysis; *ER*: Eia-Rekefjord intrusion; *Fi*: Fidsel dyke; *Ga*: Garsaknatt body chilled margin; *Ha*: Håland dyke; *Hi*: Hydra body chilled margin; *Lo*: Lomland dyke; *Te*: Tellnes dyke; *TeSa*: Tellnes satellite dyke; *Tj*: Tjörn chilled margin; *Va*: Varberg dyke; *Ve*: Vettaland dyke; *Vs*: Vaersland dyke.

least differentiated monzonorites apparently rules out that they are residual liquids after anorthosite crystallization. This conclusion is corroborated by the distinctly different isotopic signatures of monzonorites and the associated massif-type anorthosites (Demaiffe et al., 1986). Hence, it is most likely that the monzonorites represent an independent

magmatic rock series (Duchesne et al., 1974, 1985b, 1989; Demaiffe and Hertogen, 1981; Duchesne and Hertogen, 1988; Wilmart et al., in press).

An origin of the monzonorites by anhydrous partial fusion of basic rocks in the lower crust has been proposed by Duchesne et al. (1985a,b, 1989) and Demaiffe et al. (1986), the melting process being

induced by the diapiric ascent of the voluminous mantle-derived massif-type anorthosites.

This paper focuses on the so-called "Lyngdal hyperites" (LYHY) (Lavreau, 1970), two small intrusions cropping out at the extreme South of Norway, 50 km to the East of the Rogaland anorthosite complex (Fig. 1).

Hyperite is an old Swedish name for a rock composed of hypersthene, plagioclase and augite. It has always been of local application and restricted to Scandinavia. Brøgger (1934) used it restrictively for a coronitic metagabbro. As reviewed by Johannsen (1937, pp. 238), the term has been used to describe various basic rock types, such as diabase, hypersthene, gabbro and olivine gabbro.

In the Sveconorwegian province of Sweden, hyperites crop out as deformed dolerite intrusions of small extent (Lundqvist, 1980; Gower, 1985). In the Bamble-Kongsberg sector of S Norway, hyperites commonly occur as kilometer-sized syn-metamorphic gabbros, olivine gabbros, coronitic gabbros, gabbro-norites and their metamorphic equivalent amphibolites (Touret, 1969; Morton et al., 1970; Clough and Field, 1980; Starmer, 1985).

In recent studies (Falkum, 1982; Petersen, 1985; Falkum and Petersen, 1987; Barton and Van Gaans, 1988), the LYHY have been associated and compared with the Rogaland anorthosite complex, especially with the Hydra body which belongs to the monzonorite series of this complex (Demaiffe and Hertogen, 1981). To test this hypothesis, new mineralogical, geochemical and isotopic data were obtained on the LYHY.

Field and petrographic description of the Lyngdal hyperites (LYHY)

The LYHY crop out as two small ($< 1.5 \text{ km}^2$) intrusions of gabbro-noritic to monzonoritic composition (Fig. 1), located in Skoland and in the village of Lyngdal (Vest-Agder, Norway). The LYHY are emplaced as undeformed, post-tectonic bodies intruding the Sveconorwegian amphibolite facies granitic-, augen- and banded-gneisses (Falkum and Petersen, 1980; Falkum, 1982, 1985). The contact between the LYHY and gneisses is sharp and discordant. The hyperite is a dark, grey-blue, medium-grained (1 to 5 mm), homogeneous rock. Occa-

sionally large plagioclase phenocrysts (up to 5 cm) are observed.

All samples have the same mineralogy: plagioclase + orthopyroxene + clinopyroxene, with minor quantities of biotite + ilmenite + magnetite + apatite + K-feldspar + quartz + pyrite. Minute inclusions of zircon are present in the biotites of some samples. Green spinel, olivine and Opx/Fe-Ti oxide symplectite have been observed by Barton and Van Gaans (1988) in very few samples. Secondary amphibole is also present in some samples.

The rock has a subophitic texture made up of slightly zoned (see mineral chemistry section) plagioclase laths and – often poikilitic – orthopyroxene and clinopyroxene. Clinopyroxene is less abundant than orthopyroxene. Large Opx crystals are surrounded by few small grains of Cpx which could represent external granule exsolutions (Lindsley and Andersen, 1983). Cpx displays fine exsolution lamellae and Schiller inclusions. Plagioclase laths are commonly surrounded by myrmekite fringes. Quartz, K-feldspar, K-feldspar/quartz symplectitic intergrowths and apatite fill the interstices between the plagioclase laths. Biotite is a late stage mineral, surrounding oxides or occurring in dactylitic textures around pyroxenes.

The texture of the LYHY is characteristic of a magmatic liquid (unladen with crystals) which crystallized in closed-system (Petersen, 1985). Plagioclase laths crystallized first, followed by pyroxenes and oxides. The crystallization of the residual liquid gave rise to the zoned rim of the plagioclase, to the myrmekitic fringes and to the interstitial minerals. Due to the small areal extent ($< 1.5 \text{ km}^2$) of the LYHY, it is improbable that magmatic differentiation was important enough to give rise to large amounts of cumulate rocks.

Modal compositions of the LYHY fall in the fields of gabbro-norites, leuconorites and monzonorites in the Streckeisen (1974) Q-A-P diagram.

Analytical methods

Mineral compositions were determined with a CAMECA electron microprobe (CAMST, Univ. Catholique de Louvain). For each sample, several groups of minerals were analyzed in the same thin section. Feldspar (core and rim) compositions were measured. Core and rim compositions were mea-

TABLE 1

Representative microprobe analyses of pyroxenes of the LYHY

Sample	1a		2		3a		3b		7		9		11b	
	Opx	Cpx	Opx	Cpx	Opx	Cpx	Opx	Cpx	Opx	Cpx	Opx	Cpx	Opx	Cpx
SiO ₂	51.87	52.21	51.67	52.27	52.07	51.80	51.35	51.76	52.07	52.16	51.34	51.41	52.44	51.97
TiO ₂	0.09	0.18	nd	0.14	nd	0.17	nd	0.13	nd	0.12	0.04	0.29	0.09	0.17
Al ₂ O ₃	1.00	1.51	0.91	1.42	0.92	1.61	0.98	1.56	1.05	1.51	0.96	1.71	1.12	1.53
FeO	25.62	9.18	25.58	8.90	24.68	9.00	26.24	9.80	24.81	8.82	25.43	10.20	23.00	8.29
MnO	0.53	0.21	0.57	0.23	0.51	0.26	0.73	0.32	0.62	0.30	0.56	0.26	0.57	0.23
MgO	19.80	13.21	20.21	13.46	20.47	13.28	19.11	12.94	20.06	13.79	19.97	12.87	21.83	13.68
CaO	0.56	22.49	0.49	22.62	0.48	22.55	0.51	22.46	0.57	22.46	0.50	21.80	0.57	22.68
Na ₂ O	nd	0.35	nd	0.35	nd	0.37	nd	0.39	nd	0.39	nd	0.44	nd	0.47
Tot	99.47	99.34	99.43	99.39	99.13	99.04	98.92	99.36	99.18	99.55	98.80	98.98	99.62	99.02
Si	1.973	1.962	1.963	1.958	1.976	1.949	1.971	1.948	1.979	1.949	1.964	1.944	1.966	1.949
Ti	0.003	0.005		0.004		0.005		0.004		0.003	0.001	0.008	0.002	0.005
Al	0.045	0.067	0.040	0.063	0.041	0.071	0.044	0.069	0.047	0.066	0.043	0.076	0.049	0.068
Fe ³⁺	0.003	0.026	0.033	0.039	0.007	0.049	0.015	0.058	0.000	0.056	0.027	0.051	0.015	0.059
Fe ²⁺	0.812	0.263	0.780	0.240	0.777	0.234	0.827	0.251	0.789	0.220	0.786	0.271	0.706	0.201
Mn	0.017	0.007	0.018	0.007	0.016	0.008	0.024	0.010	0.020	0.009	0.018	0.008	0.018	0.007
Mg	1.123	0.740	1.144	0.752	1.158	0.745	1.094	0.726	1.136	0.768	1.139	0.726	1.220	0.765
Ca	0.023	0.905	0.020	0.908	0.019	0.909	0.021	0.906	0.023	0.899	0.021	0.883	0.023	0.911
Na		0.025		0.025		0.027		0.028		0.028		0.032		0.034
En	56.9	38.6	58.3	39.4	58.8	39.3	55.6	38.4	57.7	38.1	58.8	38.4	62.0	40.6
Fs	42.0	14.1	40.7	13.0	40.2	47.9	43.3	47.8	41.1	14.2	41.0	14.8	36.8	11.0
Wo	1.1	47.3	1.0	47.6	1.0	12.8	1.1	13.8	1.2	47.7	1.0	46.8	1.2	48.4

Total Fe as FeO; Fe²⁺ and Fe³⁺ calculated by charge balance; nd: not detected; 60 in structural formula.

TABLE 2

Representative microprobe analyses of biotites and one amphibole of the LYHY

Sample	1a	2	3a	3b	7	9	11b
	Bt	Bt	Bt	Bt	Bt	Am	Bt
SiO ₂	36.56	36.87	36.61	36.18	36.67	42.72	36.48
TiO ₂	5.07	5.40	5.49	5.40	5.60	2.17	5.16
Al ₂ O ₃	14.68	14.27	14.34	14.31	14.49	10.92	14.38
Cr ₂ O ₃	nd	nd	0.05	nd	0.13	0.21	0.13
FeO	14.14	15.93	14.81	14.73	15.02	14.09	15.81
MnO	nd	nd	0.06	nd	nd	0.06	0.09
MgO	15.00	13.61	14.01	13.80	14.78	11.98	13.62
CaO	nd	nd	nd	nd	nd	11.57	nd
Na ₂ O	nd	0.05	0.06	0.13	0.07	1.48	nd
K ₂ O	9.70	9.91	10.00	9.66	10.13	1.56	10.00
Tot	95.15	96.04	95.43	94.21	96.89	96.76	95.67
Si	5.465	5.515	5.490	5.490	5.426	6.431	5.487
Al	0.570	0.608	0.619	0.617	0.624	1.938	0.583
Ti	2.587	2.515	2.535	2.558	2.527	0.246	2.549
Cr			0.006		0.015	0.025	0.015
Fe	1.768	1.993	1.857	1.870	1.859	1.774	1.988
Mn			0.008			0.008	0.011
Mg	3.343	3.034	3.131	3.120	3.261	2.688	3.054
Ca						1.867	
Na	0.011	0.015	0.017	0.037	0.019	0.431	
K	1.850	1.890	1.913	1.870	1.912	0.300	1.919
O	22	22	22	22	22	23	22

Total Fe as FeO; nd: not detected.

sured in large and small pyroxene crystals as well as in external granule exsolutions. Crystals with abundant Schiller inclusions were avoided. The Fe²⁺/Fe³⁺ ratio of pyroxenes has been estimated by charge balance calculation.

Whole rock major and trace elements were analysed by X-ray fluorescence spectrometry (XRF) (Si, Ti, Al, Fe_{tot}, Mn, Mg, K, P on fused disks; Na, Ni, Cu, Zn, Rb, Sr, Y, Zr, Nb on powder pellets). Na, Sc, Cr, Co, Ba, Hf, Ta, REE, Th, U were measured on pressed powder pellets by standard instrumental neutron activation analyses (INAA).

Sr, Nd and Pb isotopic compositions were analyzed following the method described by Weis (1986) and Weis et al. (1987). Lead isotopic composition has been corrected for instrumental mass discrimination ($1 \pm 0.34\%$ per a.m.u.). U and Pb contents as well as the Rb content of the plagioclase phenocryst (sample 250) have been determined by isotope dilution. Nd and Sm contents obtained by INAA were used to correct the measured Nd isotopic composition for radioactive decay since formation of the rocks. The precision is about one epsilon unit.

Mineral chemistry

Eleven samples from the Skoland intrusion and two from the Lyngdal intrusion were selected for microprobe mineral chemistry determinations. Representative analyses of pyroxenes and biotite are listed in Tables 1 and 2, while average compositions of plagioclase are given for six samples in Table 3. The analysis of one amphibole is given in Table 2.

The anorthite content of plagioclase laths and phenocrysts (1–5 cm) ranges from 40 to 58% (Fig. 2) with most values between 42 and 50%. Dispersion of the values in a given sample is almost as great as the total dispersion (Fig. 2 bottom). Plagioclase laths show a slight normal zoning of 5 to 10 An%. The myrmekitic rim is more albitic (An₃₈–An₄₂) than average plagioclase laths. Phenocrysts are chemically homogeneous except in the outer 2 mm

TABLE 3

Whole rocks major and trace elements compositions of the LYHY; average compositions of plagioclase and trace element content of the plagioclase phenocryst P1250

Sample	Skoland						Lyngdal				
	1	2	3a	3b	7	9	10	250 Pl	11a	11b	19
SiO ₂	52.12	52.35	51.95	51.72	52.59	50.09	51.38	56.88	51.62	51.21	51.38
TiO ₂	2.31	2.12	2.48	2.33	1.60	2.81	1.91		2.37	2.52	2.93
Al ₂ O ₃	21.42	17.31	17.59	17.67	17.84	18.73	19.81	27.53	18.88	18.86	18.16
Fe ₂ O ₃	3.58	3.41	4.60	5.18	4.08	4.02	3.86	0.08	3.29	3.52	3.86
FeO	4.91	6.25	5.30	4.50	5.01	5.97	4.14		5.64	5.40	5.44
MnO	0.10	0.15	0.13	0.14	0.14	0.13	0.12		0.11	0.10	0.12
MgO	4.54	6.20	5.69	6.17	5.17	4.97	2.08		5.44	5.24	4.97
CaO	7.54	7.34	7.84	7.52	7.77	8.29	8.77	9.21	7.77	7.86	7.29
Na ₂ O	4.03	3.49	3.52	4.08	3.65	3.75	4.07	5.53	3.56	3.63	3.59
K ₂ O	1.02	1.34	1.24	1.12	1.27	1.04	1.60	0.47	1.10	1.10	1.34
P ₂ O ₅	0.46	0.50	0.69	0.71	0.70	0.70	0.90		0.62	0.49	0.71
Tot	102.03	100.46	101.03	100.17	99.82	100.50	98.64	99.70	100.40	99.93	99.79
Sc	13.3	16.7	15.8	12.0	15.4	15.5	13.8	0.69	13.8	13.9	15.9
Cr	84	133	84	28	73	90	3		85	87	89
Co	37.4	42.8	42.1	30.4	34.7	42.0	25.8		39.1	39.6	42.6
Ni	82	90	81	54	52	76	21		85	86	86
Cu	24	12	17	19	11	20	12		21	20	26
Zn	76	98	94	109	101	96	88		82	79	90
Rb	23	30	28	25	29	18	36	6.1	23	22	30
Sr	549	508	528	639	536	565	589	869	556	571	530
Ba	365	365	395	360	435	350	495	165	530	325	420
Y	9	29	30	25	32	24	38		23	24	30
Zr	186	204	211	177	198	199	244		174	196	203
Hf	3.28	4.23	4.02	3.24	4.09	3.68	5.20		2.97	3.30	4.10
Nb	6	7	11	9	10	8	10		9	7	8
Ta	0.77	0.77	0.75	0.74	0.69	0.68	0.91		0.57	0.66	0.78
La	15.9	19.7	19.8	16.0	22.5	16.1	25.5	2.8	15.6	15.9	20.3
Ce	37.4	46.3	46.1	37.0	51.9	38.6	57.6	5.8	33.9	37.7	48.0
Nd	21.6	27.1	27.4	22.3	31.2	24.7	36.4	2.9	19.9	21.6	28.7
Sm	5.01	6.03	6.45	5.35	7.19	5.91	8.40	0.59	4.81	4.89	6.49
Eu	1.85	2.02	2.12	1.91	2.39	2.08	2.79	0.89	1.71	1.82	2.19
Tb	0.69	0.88	0.89	0.71	0.99	0.81	1.14	0.066	0.67	0.75	0.96
Yb	1.84	2.36	2.19	1.77	2.54	1.91	2.76	0.13	1.65	1.81	2.28
Lu	0.27	0.34	0.32	0.25	0.36	0.28	0.40	0.018	0.24	0.26	0.30
Th	2.0	2.5	2.4	2.12	2.53	1.27	3.0	0.14	1.86	2.04	2.6
U	0.52	0.69	0.65	0.83	0.72	0.34	0.93	<0.15	0.47	0.61	0.66
Plagioclases											
Ab	55.1	49.8	52.8	50.4	52.2	51.5		50.6			
Or	1.9	2.0	2.0	1.8	1.7	2.4		2.8			
An	43.0	48.2	45.2	47.8	46.1	46.1		46.6			

Sample location: Fig. 1. Major elements in wt%; Na by INAA; trace elements in ppm. 250 Pl: plagioclase phenocryst of 4 cm; major elements of 250 Pl by microprobe; trace elements of 250 Pl by INAA on the same crystal; other plagioclase compositions: average of 3 up to 8 microprobe analyses.

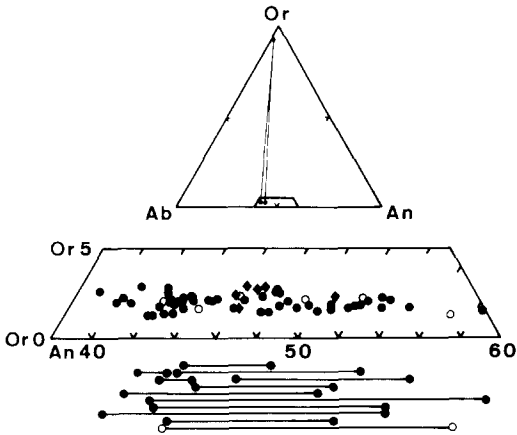


Fig. 2. Feldspar compositions. Filled circles: Skoland hyperite; open circles: Lyngdal hyperite; diamonds: plagioclase phenocryst 250Pl. Each symbol represents one analysis. The compositional range for each sample is given under the diagram by a solid line. Interstitial K-feldspar-plagioclase pairs are shown in the upper triangle.

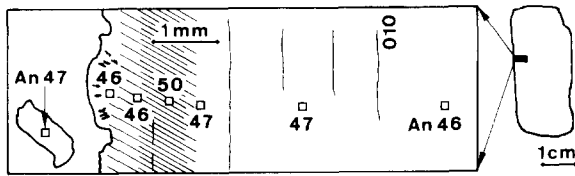


Fig. 3. Drawing showing the limited reverse zoning in the outer 2 mm of the plagioclase phenocryst P1250. Anorthite content of the phenocryst and of an adjacent (small dimension) plagioclase lath are given.

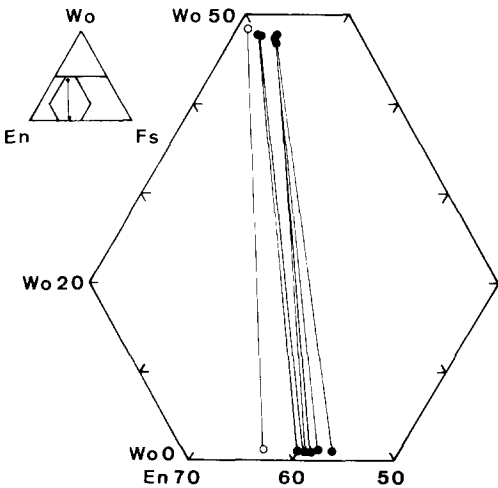


Fig. 4. Part of the pyroxene quadrilateral showing the pyroxene compositions. Representative analyses of Table 1 are plotted (same symbols as in Fig. 2).

of the crystal; an example of a reverse zoning of small amplitude in the phenocryst of sample 250 is shown in Fig. 3.

Pyroxene compositions are uniform. Orthopyroxene is hypersthene (En_{56} to En_{62}), clinopyroxene is salite ($Wo_{47.5}En_{39}Fs_{13.5}$) (Fig. 4). In a given sample, the pyroxene compositions are not correlated with the size of the crystals; no zoning is observed. Opx-Cpx equilibration temperatures range from 790 to 860°C according to the Wells (1977) geothermometer and from 680 to 820°C according to the Davidson and Lindsley (1985) geothermometer. These temperatures are not indicative of magmatic emplacement temperatures but characterise the closure of Fe-Mg-Ca exchange in the pyroxene system during the cooling (Rietmeijer, 1984). The presence of external granule exsolutions also point to pyroxene re-equilibration at subsolidus temperatures (Lindsley and Andersen, 1983).

Whole rock composition

Major and some trace elements were analysed in 18 samples of the LYHY. Ten were selected and analysed for trace elements by INAA (7 in Skoland and 3 in Lyngdal; Table 3).

Major element diagrams were used to define the

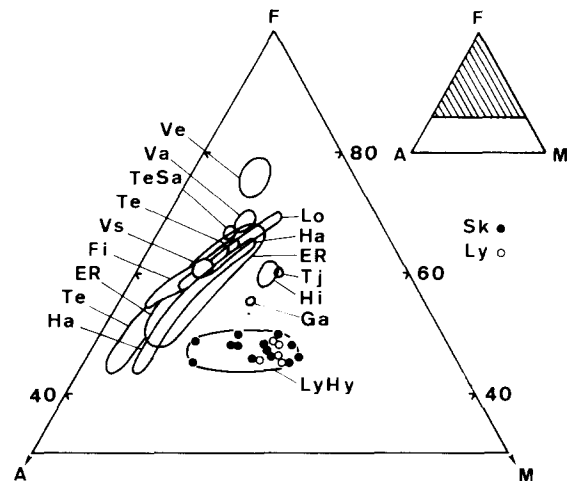


Fig. 5. Part of the AFM diagram ($A=Na_2O+K_2O$; $F=FeO_{tot}$; $M=MgO$) showing the LYHY (same symbols as in Fig. 2) and some other monzonorite occurrences of the Rogaland anorthosite complex (from Duchesne et al., 1989; abbreviations: Fig. 1).

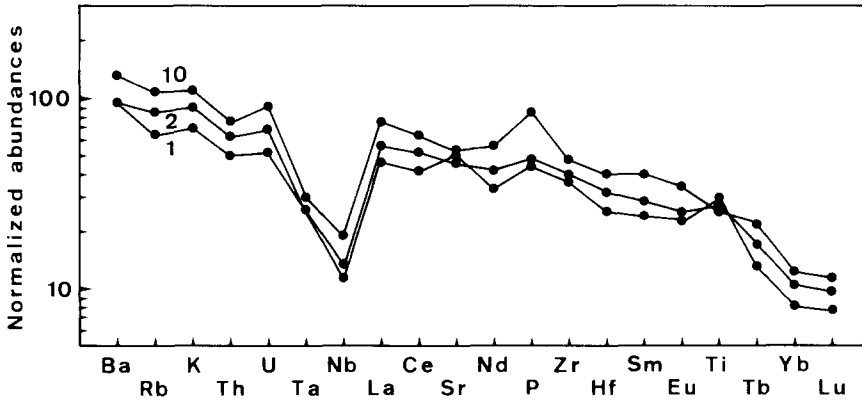


Fig. 6. Normalized incompatible elements abundances of samples 1, 2 and 10 of the LYHY (10 is the most K₂O enriched sample). Primitive mantle normalization values are taken from Wood et al. (1979), Sun (1980) and Briquieu et al. (1984).

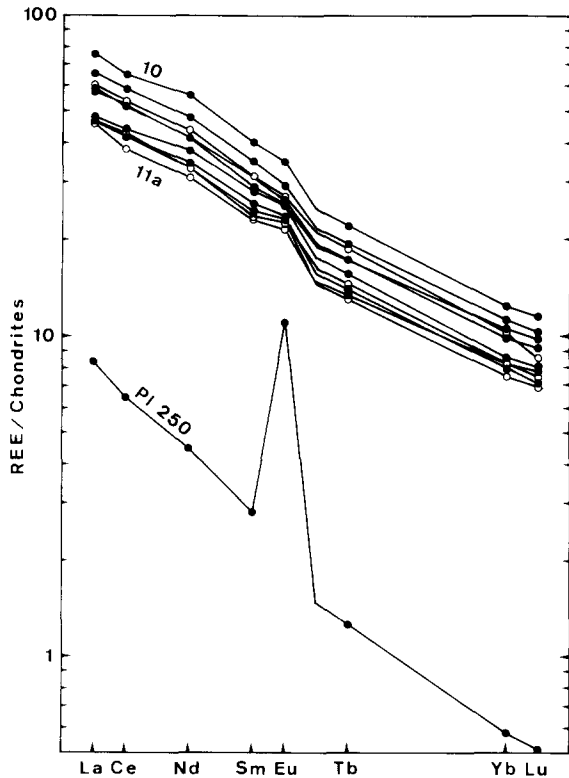


Fig. 7. Chondrite-normalized rare earth elements abundances for the hyperites (same symbols as in Fig. 2) and the plagioclase phenocryst P1250.

chemical features and affinity of the studied samples. In a R_1R_2 [$R_1 = 4Si - 11(Na + K) - 2(Fe + Ti)$, $R_2 = 6Ca + 2Mg + Al$] diagram (De la Roche et al., 1980), the LYHY plot close to the SiO₂-saturation plane, in the fields of norites–diorites and monzo-

norites. The position of the samples on the SiO₂-saturated side is compatible with the absence of olivine in nearly all the samples. The SiO₂ concentrations show very limited variation (50 to 53 wt%). K₂O contents range from 1 to 1.6%, the highest values being found in the samples enriched in interstitial minerals (Kfs, Qtz, Bt). In the Peacock (1931) diagram {log[CaO/(Na₂O+K₂O)] versus SiO₂}, the LYHY are situated at the boundary between alkali-calcic and calc-alkaline domains. The FeO_{tot}/(FeO_{tot}+MgO) ratio has a mean value of 0.66; it increases slightly from 0.6 to 0.8 in K₂O enriched samples (Fig. 5). In the AFM diagram (Fig. 5), the LYHY plot in the calc-alkaline domain. The average Al₂O₃ content of the 4 samples with the lowest K₂O content is 18.5 wt% (see Table 6; sample 1 with 21.4 wt% Al₂O₃ suggesting a local plagioclase accumulation has been discarded) which points to a high-Al affinity. However, the LYHY differ from typical high-alumina basalt compositions (Basaltic Volcanism Study Project, 1981) by their high K₂O (1.1%), TiO₂ (2.5%), P₂O₅ (0.6%) and low CaO (7.8%) contents.

Trace element data for three samples of the LYHY are presented in “spidergrams” (Fig. 6). Abundances normalized to primitive mantle decrease regularly from 100 for Ba to 10 for Lu, with pronounced negative anomalies for Ta and Nb. The LYHY are rich in REE (Fig. 7) (La_n ranges from 45 to 75) with a constant (La/Yb)_n ratio (5.9). The typically smooth patterns show only a slight positive Eu anomaly (Eu/Eu* = 1.1) in samples with the lowest REE and K₂O contents (Fig. 7). The 4cm-

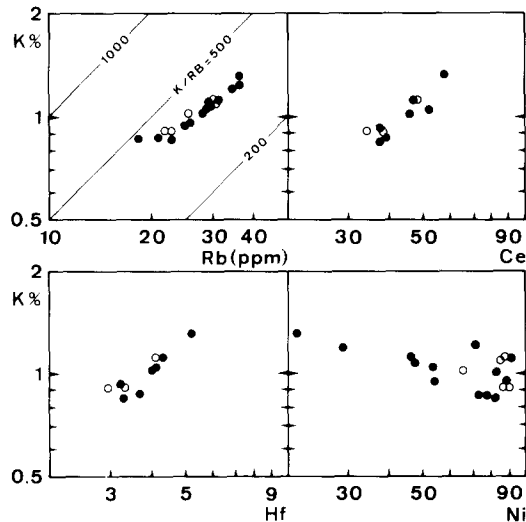


Fig. 8. Binary diagrams: K-Rb, K-Ce, K-Hf and K-Ni (same symbols as in Fig. 2).

large plagioclase phenocryst of sample 250 (Fig. 3, 250Pl in Table 3) has high Sr content (869ppm) and its REE pattern is characterized by (1) a large positive Eu-anomaly ($\text{Eu}/\text{Eu}^* = 5$), (2) low REE content ($\text{La}_n = 8.6$) and (3) a LREE enriched trend ($(\text{La}/\text{Yb})_n = 14$) (Fig. 7).

The absence of large Eu-anomalies in whole rocks precludes that the samples represent cumulates enriched in plagioclase and supports the assumption that they represent magmatic liquids.

The incompatible elements contents of the LYHY increase with increasing K_2O content (Figs. 6, 7, 8, Table 3): Rb increases from 18 to 36 ppm, Zr from 170 to 245 ppm, Hf from 3 to 5.2 ppm, Ta from 0.6 to 0.9 ppm, Ce from 34 to 58 ppm and Yb from 1.6 to 2.8 ppm. Transition elements show a concomitant decrease, e.g. Ni from 90 to 20 ppm (Fig. 8), while Sr stays nearly constant. In the K-Rb diagram, the data plot along a line corresponding to an average K/Rb ratio of 380 (Fig. 8). Samples with the lowest K and Rb contents have K/Rb ratios up to almost 500. This is due to the high modal abundance of plagioclase which is characterized by a high K/Rb ratio: (e.g. 640 in 250 Pl). Ratios of other incompatible elements are constant: $\text{Zr}/\text{Hf} = 52$, $\text{Nb}/\text{Ta} = 12$, $\text{Th}/\text{U} = 3.5$.

In bilogarithmic diagrams (Fig. 8), incompatible elements define linear arrays covering a relatively small range suggesting that some fractional crystallization occurred. The K-enriched samples repre-

sent the most differentiated liquids. Because the SiO_2 content of the LYHY is rather constant ($50 < \text{SiO}_2 < 53\%$), the fractionated mineral assemblage must have approximately the same SiO_2 content as the magmatic liquid. It probably mainly consists of plagioclase, (ortho)pyroxene and subordinate amounts of olivine and oxides. The small positive Eu-anomaly exhibited by the least evolved liquid, - i.e. those having the lowest REE content - disappears in the more evolved ones (Fig. 7). Bulk phosphorus and K contents are positively correlated: P_2O_5 increases from 0.45 to 0.9% implying that apatite did not belong to the fractionated mineral assemblage. Apatite saturation was only reached at the late stage of crystallization, which is consistent with its occurrence as an interstitial phase. This explains why REE, which have partition coefficient greater than unity for apatite (Watson and Green, 1981), largely behaved as incompatible elements during the magmatic evolution (Figs. 7 and 8).

Sr, Nd and Pb isotopic data

The Sr isotopic composition has been measured in seven samples from Skoland, three from Lyngdal (Table 4) and one plagioclase phenocryst (250Pl). In spite of the narrow range (0–0.2) of $^{87}\text{Rb}/^{86}\text{Sr}$ ratios, the samples from the Skoland hyperite including the plagioclase phenocryst, define a linear array corresponding to a good Rb-Sr isochron ($\text{MSWD} = 0.74$; Fig. 9). The calculated age is $910 \pm 82\text{Ma}$ (2σ level). The initial $^{87}\text{Sr}/^{86}\text{Sr}$ ratio deduced from the isochron is 0.7054 ± 0.0001 . In the

TABLE 4

Sr isotopic composition of the LYHY

Sample	Rb	Sr	$^{87}\text{Rb}/^{86}\text{Sr}$	$^{87}\text{Sr}/^{86}\text{Sr} \pm 2\sigma$	
250Pl	6.1*	869	0.0204	0.70565	0.00002
1	23.2	549	0.1223	0.70707	0.00002
2	30.0	508	0.1709	0.70771	0.00004
3a	28.4	527	0.1559	0.70739	0.00008
3b	24.8	639	0.1123	0.70673	0.00004
				0.70670	0.00007
7	29.2	536	0.1576	0.70753	0.00006
9	17.7	565	0.0906	0.70658	0.00006
10	36.0	589	0.1768	0.70759	0.00002
11a	23.2	556	0.1207	0.70701	0.00005
11b	22.4	571	0.1135	0.70616	0.00004
13	30.2	530	0.1649	0.70730	0.00003

*Rb of 250Pl by isotope dilution; other values by XRF.

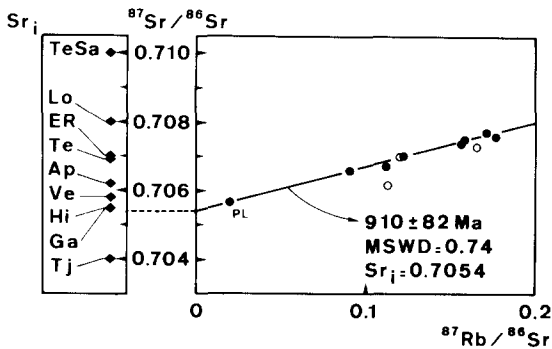


Fig. 9. $^{87}\text{Sr}/^{86}\text{Sr}$ versus $^{87}\text{Rb}/^{86}\text{Sr}$ diagram. The samples of the Skoland hyperite (filled circles) define an isochron of 910 ± 82 Ma (error at 2σ level). On the left, $^{87}\text{Sr}/^{86}\text{Sr}$ initial ratios (Sr_i) of the monzonorite occurrences of the Rogaland anorthosite complex (compilation of Duchesne et al., 1989; abbreviations: Fig. 1).

Sveconorwegian Province of South Norway (Rogaland–Vest-Agder), peak metamorphism (M2 phase of Maijer et al., 1981) has been dated at around 1000 Ma (Pasteels and Michot, 1975; Pasteels et al., 1979; Wielens et al., 1981; Demaiffe and Michot, 1985; Verschure, 1985). The intrusion age of the undeformed hyperites (910 Ma) is thus compatible with a post-tectonic emplacement.

Two of the three analysed samples of the Lyngdal hyperite fall on the same isochron. Although the third sample deviates significantly from the isochron, it is nevertheless felt that the data are strongly suggestive of a cogenetic nature of the two intrusions.

Nd and Pb isotopic compositions have been obtained on two samples of the LYHY (Table 5). ϵNd values have been calculated at 910 and 930 Ma (930 Ma = the emplacement age of related rocks in the Rogaland anorthosite complex, see next section). They range from +0.2 to +1.9 and point to a time-integrated slightly depleted source. Measured Pb isotopic compositions have been corrected for in situ decay of U during 910 and 930 Ma (Fig. 10) (the

correction is small due to low U concentrations); average initial values are 17.45 ($^{206}\text{Pb}/^{204}\text{Pb}$) and 15.51 ($^{207}\text{Pb}/^{204}\text{Pb}$).

Geochemical comparison between the Lyngdal hyperites and the monzonoritic series of the Rogaland anorthosite complex

The monzonorites associated with the Rogaland anorthosite complex are present in four different modes (Fig. 1): (1) as dykes crosscutting the massif-type anorthosite bodies: from S E to N W, the Fidsel dike (*Fi*), the Tellnes dyke (*Te*) and its satellite dyke (*TeSa*), the Håland dyke (*Ha*), the Lomland dyke (*Lo*), the Varberg dyke (*Va*), the Vaersland dyke (*Vs*) and the Vettaland dyke (*Ve*) (Duchesne et al., 1985b, 1989; Wilmart et al., in press); (2) as the undifferentiated Eia–Rekefjord intrusion (*ER*) (Michot, 1960; Wiebe, 1984); (3) as pillow-like inclusions in the Apophysis of the Bjerkreim–Sokndal lopolith (*Ap*) (Duchesne et al., 1989); (4) as differentiated intrusions which display chilled margins of monzonoritic composition and large volumes of cumulate leuconoritic material: the Hydra body (*Hi*) (Demaiffe and Hertogen, 1981), the Garsaknatt body (*Ga*) (Demaiffe, 1977) and the Bjerkreim–Sokndal lopolith. The emplacement history of the Bjerkreim–Sokndal lopolith is complex and took place in several stages (Michot, 1960; Duchesne, 1972, 1978; Rietmeijer, 1979; Duchesne et al., 1987). A chilled margin is present at Tjörn (*Tj*) (Duchesne and Hertogen, 1988). Only the chilled margins of these intrusions are considered in this study for comparison with the LYHY.

General features of the rocks of the monzonoritic series are described in Duchesne et al. (1985a, b, 1989) and Demaiffe et al. (1986). Petrographically, they range from gabbro-norites to true monzonorites (=jotunites) and to late stage charnock-

TABLE 5

Pb and Nd isotopic compositions of the LYHY

Sample	Pb	U	$^{206}\text{Pb}/^{204}\text{Pb}$	$^{207}\text{Pb}/^{204}\text{Pb}$	$^{208}\text{Pb}/^{204}\text{Pb}$	$(^{206}\text{Pb}/^{204}\text{Pb})_{930\text{Ma}}$	$(^{207}\text{Pb}/^{204}\text{Pb})_{930}$	$(^{208}\text{Pb}/^{204}\text{Pb})_{930}$	Sm	Nd	$^{147}\text{Sm}/^{144}\text{Nd}$	$^{143}\text{Nd}/^{144}\text{Nd}$	$\pm 2\sigma$	$\epsilon_{\text{Nd}}^{910\text{Ma}}$	$\epsilon_{\text{Nd}}^{930\text{Ma}}$
10	5.6	0.7	18.649	15.605	38.197	17.418	15.519	38.197	8.4	36.4	0.1395	0.51239	0.00002	1.8	1.9
11a	5.1	0.55	18.545	15.579	38.107	17.510	15.505	38.107	4.81	19.9	0.1461	0.51235	0.00004	0.2	0.4

Pb and U in ppm by isotope dilution; Sm and Nd in ppm by NAA.

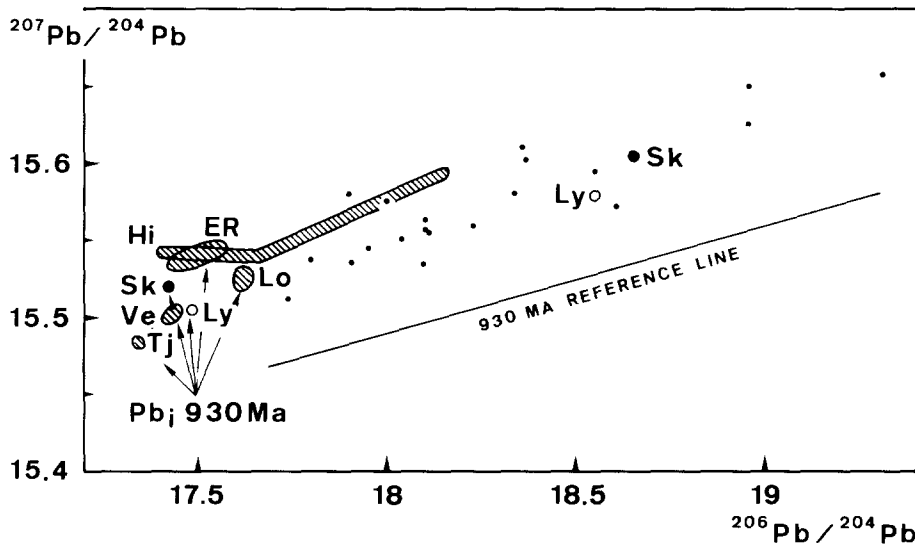


Fig. 10. $^{207}\text{Pb}/^{204}\text{Pb}$ versus $^{206}\text{Pb}/^{204}\text{Pb}$ diagram. Sk: Skoland hyperite; Ly: Lyngdal hyperite; small dots: monzonorites of the Rogaland anorthosite complex (Weis, 1986; Weis and Demaiffe, 1983). Lead initial isotopic ratios calculated at 930 Ma are shown by arrows and shaded areas for the hyperites and monzonorites.

TABLE 6

Geochemical comparison between the LYHY and published representatives of the monzonoritic series of the Rogaland anorthosite complex

Unit (a)	LYHY	Tj (6)	Hi (1,2)	Ga (3)	Lo (4)	Ha (6)	Te (7)	Va (4,6)	Ve (4,6)
SiO ₂ (b)	50–53	48–50	48–50		42–54	43–67	47–67	44–48	44–54
SiO ₂ (c)	51.2 (8)	49.4 (9)	48.0 (10)	50.2 (11)	42.7 (12)	43.8 (13)	47.3 (14)	45.9 (15)	44.2 (16)
F/F+M (d)	0.62	0.74	0.76	0.74	0.81	0.81	0.82	0.84	0.90
Al ₂ O ₃	18.5	15.8	14.2	16.9	12.2	13.5	12.8	12.6	14.1
TiO ₂	2.5	3.7	4.6	2.3	4.4	4.0	3.0	3.8	3.0
P ₂ O ₅	0.6	0.7	0.8	1.2	3.4	3.3	2.7	2.7	2.4
Cr (e)	73	28	38		3		2	3	1
Rb	22	17	19	23	5	4	16	11	4
K/Rb	416	470	460	444	1460	2120	1160	1330	1490
La _n	47	70	89	120	125	118	161	164	150
(La/Yb) _n	5.9	7.9	6.2	6.3	10	13.3	12.1	8.8	7.5
Eu/Eu*	1.1	1.1	0.9	0.9	1.1	1.3	1.1	1.3	0.9
Zr/Hf	57	44	35		22	42	40	39	48
Sr _i	0.7054	0.704	0.7055	0.7055	0.708	0.7067	0.7069		0.7058
Pb _i (f)	15.51	15.48	15.56		15.53				15.50
εNd _i	1.1		2.7 (5)						

a: abbreviations: Fig. 1; b: SiO₂ range; c: SiO₂ and other geochemical parameters: representative analysis of the least differentiated sample of each unit; major elements in wt%; d: F/F+M = FeO_t/FeO_t + MgO; e: Cr and Rb in ppm; f: Pb_i = average ($^{207}\text{Pb}/^{204}\text{Pb}$)_{930Ma}, data of Weis, 1986.

1: Duchesne et al., 1974; 2: Demaiffe and Hertogen, 1981; 3: Demaiffe, 1977; 4: Duchesne et al., 1985b; 5: Demaiffe et al., 1986; 6: Duchesne et al., 1989; 7: Wilmart et al., in press; 8: average of samples 3b, 9, 11a, 11b; 9: sample 80123; 10: sample 7020; 11: sample 411/2; 12: sample 66175; 13: sample 81323; 14: sample 7252; 15: sample 7520; 16: sample 7529.

ites in some occurrences. The texture is generally subophitic. They all contain plagioclase, orthopyroxene, clinopyroxene, hemo-ilmenite, magnetite and apatite. The Hidra and Garsaknatt chilled margins locally contain plagioclase phenocrysts (An₄₃–An₄₈; Duchesne et al., 1974; Demaiffe, 1977).

The Rogaland monzonorites are of alkali-calcic

affinity; the SiO₂ and Al₂O₃ contents are in the range 43–55% SiO₂ (up to 67% for the minor late stage charnockitic facies) and 12–17% Al₂O₃. The monzonorites are characterized by high FeO_{tot}, TiO₂ and P₂O₅ contents. Important geochemical parameters of representative samples of eight well-studied monzonorite occurrences are presented in Table 6.

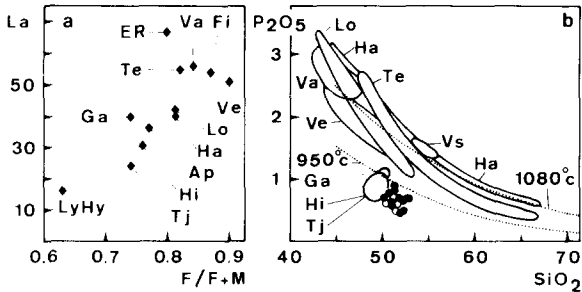


Fig. 11. a) La- $F/F+M$ diagram showing the positive correlation between La content and $F/F+M$ ratio of the least differentiated samples of the Rogaland monzonorites.

b). P_2O_5 - SiO_2 diagrams showing the LYHY (same symbols as in Fig. 2) and the Rogaland monzonorites (from Duchesne et al., 1989; abbreviations: Fig. 1). The 950 and 1080°C-7.5 Kbar apatite saturation curves are shown (Green and Watson, 1982). The trends of different Fe-rich monzonorites ($F/F+M > 0.8$) are situated along the 1080°C saturation curve and thus represent apatite-saturated magmas while magnesian monzonorites ($F/F+M < 0.8$) are plotted below the 950°C saturation curve and thus do not represent saturated magmas.

The $FeO_{tot}/FeO_{tot}+MgO$ ($F/F+M$) ratio of the different monzonoritic occurrences show a regional increase towards the center of the anorthosite complex. The monzonorites can be subdivided in three groups on the basis of increasing ratio (Figs. 1, 5): (1) those located close to the outer contact with the anorthosite (Hi, Tj, Ga, Ap) have $F/F+M$ ratios in the range 0.74 to 0.77; (2) the E-R intrusion and the main dykes crosscutting the anorthosites have higher ratios, in the range 0.80 to 0.87 and (3) the Vettaland dyke (Ve), situated in the central part of the Egersund-Ogna anorthosite has an extreme ratio of 0.90. This increase in $F/F+M$ ratio is accompanied by other geochemical variations (Table 6). The Cr content decreases from 38 ppm in Hydra to less than 5 ppm in the Fe-rich monzonorites (groups 2 and 3), while Zn content increases from 130 to 250 ppm. The whole rock REE content also grossly increases with increasing $F/F+M$ ratio (Fig. 11). The K/Rb ratio displays a sudden increase for a $F/F+M$ ratio of 0.8: it is situated in the range 400–500 for the Hi, Tj and Ga chilled margins and is higher than 1000 for all the Fe-rich monzonorites of groups 2 and 3, pointing to a strongly Rb-depleted nature. The spidergrams also show important variations: the Fe-rich monzonorites display large negative anomalies in Rb, Th, Nb-Ta, Sr, Hf-Zr and Ti while, in contrast, Hi and Tj chilled mar-

gins are characterized by smooth spidergrams with less pronounced troughs.

U/Pb zircon geochronology (Pasteels et al., 1979) shows that the monzonorites were emplaced in the short time span of 950 to 930 Ma. The Rb/Sr isochron obtained for the Tellnes main dyke gives an age of 925 ± 21 Ma (Wilmart et al., in press). The age of 910 ± 82 Ma obtained for the LYHY is, within errors, in the same range.

There are two significant major element geochemical differences between the LYHY and the monzonorites (Table 6): (1) the LYHY have higher Al_2O_3 content ($Al_2O_3 = 18.5\%$) than the monzonorites ($12\% < Al_2O_3 < 17\%$); (2) the LYHY do not display a strong Fe enrichment; the FeO_{tot} is low (9%) with respect to the range of values of the monzonorites (11.5–20%) and, consequently, the $F/F+M$ ratio of LYHY is lower (0.62) than in the monzonorites (0.74–0.90) (Figs. 1, 5).

In spite of those differences, the LYHY nevertheless display many similarities with the monzonorites: (1) Anorthite content of the plagioclase in the range 40–58% and presence of plagioclase phenocrysts; (2) enrichment in TiO_2 , P_2O_5 and K_2O ; (3) comparable REE pattern [$(La/Yb)_n$ ratio of 5.9, no Eu anomaly]; (4) Sr isotopic initial ratio comparable to those of Hydra (0.7055), Garsaknatt (0.7055) and Tjörn (0.704) chilled margins (Fig. 9); (5) Pb isotopic initial ratios in the range of those of the monzonorites (Fig. 10); (6) slightly positive ϵNd values like the Hydra chilled margin (Demaiffe et al., 1986, Demaiffe, unpubl.). The isotopic data show that the monzonorites and the LYHY derive from the same isotopic reservoir.

In the LYHY, apatite is a late stage interstitial mineral and the P_2O_5 content increases from 0.46 to 0.9% with increasing differentiation. The LYHY thus do not represent apatite-saturated liquids. In the P_2O_5 - SiO_2 diagram (Fig. 11), the LYHY, like the Hi, Tj and Ga chilled margins, indeed plot beneath the apatite saturation curve of 950°C-7.5 kbar (Green and Watson, 1982). Conversely, in the Fe-rich ($F/F+M > 0.8$) monzonorites (groups 2 and 3), the P_2O_5 content is generally high ($> 2\%$) in the least differentiated samples and decreases with increasing differentiation. Those rocks are situated along the 1080°C-7.5 kbar saturation curve and thus represent apatite saturated liquids from the beginning of the crystallization. In those rocks, apatite is a liquidus phase controlling the decrease of

P_2O_5 and REE during the fractional crystallization process (Wilmart, 1988; Wilmart et al., in press).

Discussion: a possible link between monzonorites and the Lyngdal hyperites

A major conclusion of the study of the Rogaland monzonoritic series (Duchesne et al., 1989) is that, in spite of many common features, the different occurrences (Fig. 1) are characterized by their own geochemical and isotopic signatures. The Sr initial isotopic composition varies from 0.704 to 0.710 (Fig. 9), but is generally constant within a given occurrence. These various Sr initial ratios are not correlated with the content of elements generally enriched in middle and upper crustal material (K, Rb, Ba, Th, U,...). This implies that the observed isotopic variations do not result from significant crustal contamination during emplacement and crystallization. The isotopic variability is a primary feature implying that each monzonorite occurrence represents a distinct magma batch resulting from the partial melting of an isotopically distinct source. As a matter of fact, the geochemical diversity of the monzonorites can not be explained by a fractional crystallization process of a single parental magma nor by the partial melting of a single source (Duchesne et al., 1989).

The observed variation of the $F/F+M$ ratios of the monzonorite occurrences (Fig. 1) and the possible link between these monzonorites and the LYHY can nevertheless be interpreted in a qualitative way. The compositional similarity between the Fe-rich monzonorites and the experimental (Baker and Egger, 1987) glasses obtained by low degree (6%) of partial melting of high-Al basalts at 8 Kbar under anhydrous conditions was noticed by Duchesne et al. (1989). They tentatively deduced that Fe-rich monzonorites could result from the low degree of partial melting of basic rocks situated in the lower crust (granulite facies), the heat for which being supplied by the ascent of the mantle-derived massif-type anorthosites. With increasing melting degree, the $F/F+M$ ratio as well as the TiO_2 and P_2O_5 contents of the experimentally produced glasses decrease (Baker and Egger, 1987; Meen, 1987). This suggests that the most Mg-rich ($F/F+M < 0.8$) monzonorites (Hi, Tj and Ga chilled margins) would result from higher degrees of melt-

ing than the Fe-rich monzonorites. The LYHY which still have a lower $F/F+M$ ratio, could tentatively be interpreted as an Fe-poor (or Mg-rich) end-member of the monzonoritic magmatism, cropping out 50 Km to the East of the anorthosite complex and resulting from still larger degree of melting. Some evidence supports this assumption: (1) on average, the Fe-rich monzonorites have higher REE content than Mg-rich monzonorites, the LYHY having the lowest REE content (Fig. 11); this is consistent with the behaviour of REE as incompatible elements during partial melting; (2) the LYHY have the highest Ni and Cr content among all the analysed monzonorites (Table 6); (3) apatite is a residual phase in the source of the Fe-rich monzonorites but not of more magnesian ones (Fig. 11); (4) the more irregular trace element spidergrams of the Fe-rich monzonorites point to a more diversified residual mineralogy, which is compatible with low degrees of fusion.

Relative to Fe-rich monzonorites, the magnesian varieties – and more particularly the LYHY – could thus represent partial melts generated either at higher temperatures (at a deeper level) or at the same temperatures (at the same level) but under less anhydrous conditions.

Acknowledgements

The whole rock major elements analyses were obtained at the Collectif de Géochimie (Univ. de Liège) and the microprobe data at the C.A.M.S.T. (Univ. Catholique de Louvain); thank are due to G. Bologne and J. Wauthier. Ch. Gilson (M.R.A.C. Tervuren), C. Chaval and J.P. Mennessier are thanked for technical assistance.

We wish to thank Drs. J.C. Duchesne and F. Rietmeijer for their constructive critical comments and suggestions.

References

- Baker, D.R. and Egger, D.H., 1987. Compositions of anhydrous and hydrous melts coexisting with plagioclase, augite, and olivine or low-Ca pyroxene from 1 atm to 8 kbar: application to the Aleutian volcanic center of Atka. *Am. Mineral.*, 72: 12–28.
- Barton, M. and Van Gaans, C., 1988. Formation of orthopyroxene–Fe–Ti–oxide symplectites in Precambrian intru-

- sives, Rogaland, southwestern Norway. *Am. Mineral.*, 73: 1046–1059.
- Basaltic Volcanism Study Project, 1981. *Basaltic volcanism on the terrestrial planets*. Pergamon Press, Oxford, 1286 pp.
- Briqueu, L., Bougault, H. and Joron, J.L., 1984. Quantification of Nb, Ta, Ti and V anomalies in magmas associated with subduction zones: petrogenetic implications. *Earth Planet. Sci. Lett.*, 68: 297–308.
- Brøgger, W.C., 1934. On several Archean rocks from the South coast of Norway. *Vid. Selsk., Skr. 1, Mat. Nat. Kl.*, nb.8 1933 and nb.1 1934.
- Clough, P. and Field, D., 1980. Chemical variation in metabasites from a Proterozoic amphibolite–granulite transition zone, South Norway. *Contrib. Mineral. Petrol.*, 73: 277–286.
- Davidson, P.M. and Lindsley, D.H., 1985. Thermodynamic analysis of quadrilateral pyroxenes. Part 2: Model calibration from experiments and applications to geothermometry. *Contrib. Mineral. Petrol.*, 91: 390–404.
- De la Roche, H., Leterrier, J., Granclaude, P. and Marchal, M., 1980. A classification of volcanic and plutonic rocks using R1R2 diagram and major-element analyses. Its relationships with current nomenclature. *Chem. Geol.*, 29: 183–210.
- Demaiffe, D., 1977. De l'origine des anorthosites. *Petrologie, géochimie et géochimie isotopique des massifs anorthositiques d'Hidra et de Garsaknatt (Rogaland, Norvège méridionale)*. Thesis, Univ. Bruxelles, 362 pp.
- Demaiffe, D. and Hertogen, J., 1981. Rare earth element geochemistry and strontium isotopic composition of a massif-type anorthositic–charnockitic body: the Hidra Massif (Rogaland, S W Norway). *Geochim. Cosmochim. Acta*, 45: 1545–1561.
- Demaiffe, D. and Michot, J., 1985. Isotope geochronology of the Proterozoic crustal segment of southern Norway: a review. In: A.C. Tobi and J. Touret (Editors), *The deep Proterozoic crust in the North Atlantic Provinces*. Reidel, Dordrecht, pp. 411–434.
- Demaiffe, D., Weis, D., Michot, J. and Duchesne, J.C., 1986. Isotopic constraints on the genesis of the Rogaland anorthositic suite (Southwest Norway). *Chem. Geol.*, 57: 167–179.
- Duchesne, J.C., 1972. Iron-titanium minerals in the Bjerkreim–Sokndal massif, South-Western Norway. *J. Petrol.*, 13: 57–81.
- Duchesne, J.C., 1978. Quantitative modeling of Sr, Ca, Rb and K in the Bjerkreim–Sokndal layered lopolith (S.W. Norway). *Contrib. Mineral. Petrol.*, 66: 175–184.
- Duchesne, J.C., Denoiseux, B. and Hertogen, J., 1987. The norite–mangerite relationships in the Bjerkreim–Sokndal layered lopolith (Southwest Norway). *Lithos*, 20: 1–17.
- Duchesne, J.C. and Hertogen, J., 1988. Le magma parental du lopolithe de Bjerkreim–Sokndal (Norvège méridionale). *C.R. Acad. Sci. Paris*, 306, série 2: 45–48.
- Duchesne, J.C., Maquil, R. and Demaiffe, D., 1985a. The Rogaland anorthosites: facts and speculations. In: A.C. Tobi and J. Touret (Editors), *The deep Proterozoic crust in the North Atlantic Provinces*. Reidel, Dordrecht, pp. 449–476.
- Duchesne, J.C., Michot, J., 1987. The Rogaland intrusive masses: introduction. In: C. Majjer and P. Padget (Editors), *The geology of Southernmost Norway*. *Nor. Geol. Unders. Spec. Publ.1*, pp. 48–59.
- Duchesne, J.C., Roelandts, I., Demaiffe, D., Hertogen, J., Gijbels, R. and de Winter, J., 1974. Rare earth data on monzonoritic rocks related to anorthosites and their bearing on the nature of the parental magma of the anorthositic series. *Earth Planet. Sci. Lett.*, 24: 325–335.
- Duchesne, J.C., Roelandts, I., Demaiffe, D. and Weis, D., 1985b. Petrogenesis of monzonoritic dykes in the Egersund–Ogna anorthosite (Rogaland, S.W. Norway): trace elements and isotopic (Sr,Pb) constraints. *Contrib. Mineral. Petrol.*, 90: 214–225.
- Duchesne, J.C., Wilmart, E., Demaiffe, D. and Hertogen, J., 1989. Monzonorites from Rogaland (Southwest Norway): a series of rocks coeval but not comagmatic with massif-type anorthosites. *Precamb. Res.*, 45: 111–128.
- Falkum, T., 1982. *Geologisk kart over Norge, berggrunnskart Mandal 1: 250000*. Norges Geol. Unders.
- Falkum, T., 1985. Geotectonic evolution of southern Scandinavia in light of a late-Proterozoic plate collision. In: A.C. Tobi and J. Touret (Editors), *The deep Proterozoic crust in the North Atlantic Provinces*. Reidel, Dordrecht, pp. 309–322.
- Falkum, T. and Petersen, J., 1980. The Sveconorwegian orogenic belt, a case of late-Proterozoic plate-collision. *Geol. Rundsch.*, 69: 622–647.
- Falkum, T. and Petersen, J., 1987. The Agder migmatitic gneiss complex. In: C. Majjer and P. Padget (Editors), *The geology of Southernmost Norway*. *Nor. Geol. Unders. Spec. Publ.1*, pp. 40–47.
- Falkum, T., Wilson, J.R., Petersen, J. and Zimmermann, H.D., 1979. The intrusive granites of the Farsund area, south Norway: their interrelations and relations with the Precambrian metamorphic envelope. *Nor. Geol. Tidsskr.*, 59: 125–139.
- Gower, C.F., 1985. Correlations between the Grenville Province and Sveconorwegian orogenic belt – implications for proterozoic evolution of the southern margins of the Canadian and Baltic Shields. In: A.C. Tobi and J. Touret (Editors), *The deep Proterozoic crust in the North Atlantic Provinces*. Reidel, Dordrecht, pp. 247–258.
- Green, T.H. and Watson, B.E., 1982. Crystallization of apatite in natural magmas under high pressure, hydrous conditions, with particular reference to “orogenic” rock series. *Contrib. Mineral. Petrol.*, 79: 96–105.
- Johanssen, A., 1937. *A descriptive petrography of the igneous rocks*, Vol. 3. Univ. Chicago Press, Chicago, 360 pp.
- Lavreau, J., 1970. Pyroxene relations in a hyperite near Lyngdal, Norway. *Nor. Geol. Tidsskr.*, 50: 333–340.
- Lindsley, D.H. and Andersen, D.J., 1983. A two-pyroxene thermometer. *Proc. Lunar Conf. J. Geophys. Res.*, 88: A887–A906.
- Lundqvist, T., 1980. The Precambrian of Sweden. In: *Geology of the European countries*. 26th Int. Geol. Congr., Paris 1980, Dunod, pp. 219–271.
- Majjer, C., Andriessen, P., Hebeda, E., Jansen, J. and Verschure, R., 1981. Osumilite, an approximately 970 Ma old

- high-temperature index mineral of the granulite-facies metamorphism in Rogaland, S.W. Norway. *Geol. Mijnbouw*, 60: 267–272.
- Meen, J.K., 1987. Formation of shoshonites from calc-alkaline basalt magmas: geochemical and experimental constraints from the type locality. *Contrib. Mineral. Petrol.*, 97: 333–351.
- Michot, P., 1960. La géologie de la catazone: le problème des anorthosites, la palingénèse basique et la tectonique catazonale dans le Rogaland méridional, (Norvège). *Int. Geol. Congr., Oslo 1960, guide de l'excursion A 9. Nor. Geol. Unders.*, 60 pp.
- Michot, J. and Michot, P., 1969. The problem of the anorthosites. The South Rogaland igneous complex (South Western Norway). In: Y.W. Isachsen (Editor) *Origin of anorthosites and related rocks*. N.Y. Mus. Sci. Serv., 18: 399–410.
- Morton, R.D., Batey, R. and O'Nions, R.K., 1970. Geological investigations in the Bamble Sector of the Fennoscandian Shield. South Norway. *Nor. Geol. Unders.*, 263: 1–72.
- Pasteels, P., Demaiffe, D. and Michot, J., 1979. U–Pb and Rb–Sr geochronology of the eastern part of the South Rogaland igneous complex, southern Norway. *Lithos*, 12: 199–208.
- Pasteels, P. and Michot, J., 1975. Geochronologic investigation of the metamorphic terrain of southwestern Norway. *Nor. Geol. Tidssk.*, 55: 111–134.
- Peacock, M.A., 1931. Classification of igneous rock series. *J. Geol.*, 39: 54–67.
- Petersen, J.S., 1985. The directional solidification of silicate melts: crystallization kinetics and macrosegregation. *K. Dan. Vidensk. Sekt. Mat. FysMedd.*, 41: 338–398.
- Rietmeijer, F.J., 1979. Pyroxenes from iron-rich igneous rocks in Rogaland, S.W. Norway. Thesis Univ. Utrecht, 340 pp. Unpublished.
- Rietmeijer, F.J., 1984. Pyroxene (re)-equilibration in the Precambrian terrain of S.W. Norway between 1030–990 Ma and reinterpretation of events during regional cooling (M3 stage). *Nor. Geol. Tidsskr.*, 64: 7–20.
- Starmér, I.C., 1985. The evolution of the South Norwegian Proterozoic as revealed by the major and mega-tectonics of the Kongsberg and Bamble sectors. In: A.C. Tobi and J. Touret (Editors), *The deep Proterozoic crust in the North Atlantic Provinces*. Reidel, Dordrecht, pp. 259–290.
- Streckeisen, A., 1974. How should charnockitic rocks be named? In: J. Belliere and J.C. Duchesne (Editors), *Géologie des domaines cristallins*. Soc. Geol. Belg., Liège, pp. 267–288.
- Sun, S.S., 1980. Lead isotopic study of young volcanic rocks from mid-oceanic ridges, ocean island and island arcs. *Philos. Trans. R. Soc. London, Ser. A*, 297: 409–445.
- Touret, J., 1969. Le socle Précambrien de la Norvège méridionale (région de Vegårshei-Gjerstad). Thesis Univ. Nancy, 3 vol.
- Verschure, R.H., 1985. Geochronological framework for the Late-Proterozoic evolution of the Baltic Shield in South Scandinavia. In: A.C. Tobi and J. Touret (Editors), *The deep Proterozoic crust in the North Atlantic Provinces*. Reidel, Dordrecht, pp. 381–410.
- Watson, B.E. and Green, T.H., 1981. Apatite/liquid partition coefficients for the rare earth elements and strontium. *Earth Planet. Sci. Lett.*, 56: 405–421.
- Weis, D., 1986. Genetic implications of Pb isotopic geochemistry in the Rogaland anorthositic complex (Southwest Norway). *Chem. Geol.*, 57: 181–199.
- Weis, D. and Demaiffe, D., 1983. Pb isotope geochemistry of a massif-type anorthositic–charnockitic body: the Hidra Massif (Rogaland, S.W. Norway). *Geochim. Cosmochim. Acta*, 47: 1405–1413.
- Weis, D., Demaiffe, D., Cauet, S. and Javoy, M., 1987. Sr, Nd, O and H isotopic ratios in Ascension lavas and plutonic inclusions: cogenetic origin. *Earth Planet. Sci. Lett.*, 82: 255–268.
- Wells, P.R., 1977. Pyroxene thermometry in simple and complex systems. *Contrib. Mineral. Petrol.*, 62: 129–139.
- Wiebe, R.A., 1984. Commingling of magmas in the Bjerkrem-Sokndal lopolith (Southwest Norway): evidence for the compositions of residual liquids. *Lithos*, 17: 171–188.
- Wielens, J., Andriessen, P., Boelrijk, N., Hebeda, E., Priem, H., Verdurmen, E. and Verschure, R., 1981. Isotope geochronology in the high-grade metamorphic Precambrian of southwestern Norway: new data and reinterpretations. *Nor. Geol. Unders.*, 359: 1–30.
- Wilmart, E., 1988. Etude géochimique des charnockites de Rogaland (Norvège méridionale). Thesis Univ. Paris 6, 342 pp.
- Wilmart, E., Demaiffe, D. and Duchesne, J.C., 1990. Geochemical constraints on the genesis of the Tellnes ilmenite deposit and related rocks (S.W. Norway). *Econ. Geol.*, 84: in press.
- Wood, D.A., Joron, J.-L. and Treuil, M., 1979. A reappraisal of the use of trace elements to classify and discriminate between magma series erupted in different tectonic settings. *Earth Planet. Sci. Lett.*, 45: 326–336.